View metadata, citation and similar papers at core.ac.uk

brought to you by CORE

provided by University of Richmond

University of Richmond
UR Scholarship Repository

Chemistry Faculty Publications | Chemistry

2013

Theoretical design of stable small aluminium-magnesium binary clusters

Edison Osorio

Alejandro Vasquez

Elizabeth Florez

Fanor Mondragon

Kelling J. Donald
University of Richmond, kdonald@richmond.edu

See next page for additional authors

Follow this and additional works at: http://scholarship.richmond.edu/chemistry-faculty-publications

Part of the Other Chemistry Commons

Recommended Citation

Osorio, Edison, Alejandro Vasquez, Elizabeth Florez, Fanor Mondragon, Keilling J. Donald, and William Tiznado. "Theoretical Design of Stable Small Aluminium–magnesium Binary Clusters." *Physical Chemistry, Chemical Physics* 15 (2013): 2222-229. doi:10.1039/c2cp42015e.

This Article is brought to you for free and open access by the Chemistry at UR Scholarship Repository. It has been accepted for inclusion in Chemistry Faculty Publications by an authorized administrator of UR Scholarship Repository. For more information, please contact scholarshiprepository@richmond.edu.

Authors
Edison Osorio, Alejandro Vasquez, Elizabeth Florez, Fanor Mondragon, Kelling J. Donald, and William Tiznado

This article is available at UR Scholarship Repository: http://scholarship.richmond.edu/chemistry-faculty-publications/41

PCCP

RSC Publishing

PAPER

View Article Online
View Journal | View Issue

Theoretical design of stable small aluminium–magnesium binary clusters†

Cite this: *Phys. Chem. Chem. Phys.*, 2013, **15**, 2222

Edison Osorio,*[ab] Alejandro Vasquez,[a] Elizabeth Florez,[c] Fanor Mondragon,[d] Kelling J. Donald*[e] and William Tiznado*[a]

Received 15th June 2012,
Accepted 6th September 2012

DOI: 10.1039/c2cp42015e

www.rsc.org/pccp

We explore in detail the potential energy surfaces of the Al_xMg_y (x, y = 1–4) systems as case studies to test the utility and limitations of simple rules based on electron counts and the phenomenological shell model (PSM) for bimetallic clusters. We find that it is feasible to design stable structures that are members of this set of small Al–Mg binary clusters, using simple electron count rules, including the classical $4n + 2$ Hückel model, and the most recently proposed PSM. The thermodynamic stability of the title compounds has been evaluated using several different descriptors, including the fragmentation energies and the electronic structure of the systems. Three stable systems emerge from the analysis: the Al_4Mg, Al_2Mg_2 and Al_4Mg_4 clusters. The relative stability of Al_4Mg is explained by the stability of the Al_4^{2-} subunit to which the Mg atom donates its electrons. Here the Mg^{2+} sits above the aromatic 10 π-electron Al_4^{2-} planar ring. The Al_2Mg_2 and Al_4Mg_4 clusters present more complicated 3D structures, and their stabilities are rationalized as a consequence of their closed shell nature in the PSM, with 10 and 20 itinerant electrons, respectively.

Introduction

There has been considerable interest over the past few decades in the study of pure and doped metal clusters. In particular, mixed-metal systems provide particularly good test sets for models that purport to explain the often unexpected stability and reactivity patterns present among atomic clusters with certain numbers of the constituent atoms. The potential utility of stable heteroatomic metal clusters as basic units in building specialized materials with tailored properties appears to be an attractive proposition as well.[1–4] Mixed metal (inter-metallic and alloy) systems are known to have modified and often desirable properties relative to the pure phases of the individual metal, including improved corrosion resistance, low density and malleability. Pure aluminium inherently has several of these advantages over other pure metals. However, even those characteristics can be improved in Al by doping to a small extent with other metals. The potential utility of Mg as a dopant has been examined by Varano *et al.* in 2010, for example.[5]

The arrangement of electrons that determines the properties of a compound in chemistry is often represented by the electron configuration, and there are several simple models used to interpret and predict stability due to that configuration. For example, simple electron count rules are used to describe aromatic compounds; the most popular is the Hückel $(4n + 2)$ rule,[6–8] which has been used typically to describe aromaticity in planar cyclic hydrocarbons (annulenes) and has been employed more recently to describe aromaticity and consequently stability in even metallic clusters, like Al_4^{2-}.[9] The Hückel model has also been applied to three-dimensional systems, such as fullerenes:[10] see, for example, the electron count rules that have been formulated by Hirsch *et al.*[11] One more general model, which in principle takes account of planar and spherical aromaticity, is the phenomenological shell model (PSM). The main assumption of this model is that itinerant electrons in a cluster are confined in a box according to the shape of the cluster. So, a three-dimensional system approximating a spherical shape should present relatively high stability when N = 8, 18, 20, 34, 40, 58,... Where N is the number of itinerant or valence electrons in the molecular system.[12]

Recently, we designed theoretically a set of stable silicon–lithium clusters, $Si_5Li_7^+$ (D_{5h}) and Si_4Li_4 (T_d), for which the stability was explained using planar aromaticity rules and PSM, respectively.[13a,b] That study convinced us that with the proper

[a] *Universidad Andres Bello, Facultad Ciencias Exactas, Departamento de Ciencias Químicas, Av. República 275, Santiago, Chile. E-mail: ed.osorio@uandresbello.edu, wtiznado@unab.cl*
[b] *Centro de Bioinformática y Simulación Molecular, Universidad de Talca, 2 Norte 685, Casilla 721, Talca, Chile*
[c] *Department of Basic Sciences, University of Medellin, A.A 1226, Medellín, Colombia*
[d] *Institute of Chemistry, University of Antioquia, A.A. 1226, Medellín, Colombia*
[e] *Department of Chemistry, Gottwald Center for the Sciences, University of Richmond, Richmond, Virginia 23173, USA. E-mail: kdonald@richmond.edu*

† Electronic supplementary information (ESI) available. See DOI: 10.1039/c2cp42015e

This journal is © the Owner Societies 2013

use of these simple electrons count rules, it is possible to predict the appropriate stoichiometric combination of pairs of elements to build stable heteronuclear clusters. However, for clusters, these rules are limited. In the case of Si_6Li_6, which, as a system isovalent with benzene, satisfies the $4n + 2$ rule for aromaticity, the isomer with a hexagonal Si_6 ring surrounded by six terminal Si–Li single bonds is not the thermodynamically preferred option.[13c] Experimentally, atomic clusters are produced in the gas-phase under "annealing" conditions, which tend to privilege the lowest energy isomers. So, for clusters, experimental confirmation would be anticipated for only the lowest energy isomers. An important contribution that computational chemistry makes, therefore, is to contribute to a knowledge of what isomers are energetically feasible, and an understanding of why that is so.

In this paper, we propose that with the proper stoichiometric combinations of Al and Mg atoms, it is possible to generate small and relatively stable clusters following the electron counting rules mentioned in the preceding paragraphs ($4n + 2$ and PSM). The proposed clusters all fall within the Al_xMg_y (x, y = 1–4) series. The most viable candidate for a planar-aromatic cluster within this series is the Al_4Mg (C_{4v}), which is expected to contain the Al_4^{2-} aromatic ring, which has been previously reported by Mandado *et al.*[14] The three-dimensional clusters that could be stable according to PSM would be: Al_2Mg_2 and Al_4Mg_4 with 10 and 20 itinerant electrons, respectively. In addition to the thermodynamic stability of the complexes, we analyze the electronic structure and the bonding patterns of the selected group of Al–Mg clusters. Our results suggest that it is feasible to design stable clusters by following as our preliminary guide very simple electron counting rules. In particular, we found that the Al_4Mg_4 (D_{2d}) cluster presents high relative stability and should be a good candidate for experimental synthesis. Additionally, predictive calculations of the vertical electron detachment energies are reported for the anionic species $Al_4Mg_4^-$, since in the most reliable experiments on atomic clusters the charged species are relatively easily generated, detected, and studied.

Computational details

The potential energy surfaces of the title compounds have been surveyed in detail employing the gradient embedded genetic algorithm (GEGA) program.[15–17] All of these GEGA calculations were done using the B3LYP[18,19] functional in conjunction with the Stuttgart–Dresden pseudopotentials and their respective basis sets (SDD).[20,21] The geometries and harmonic frequencies were recalculated for all the title clusters at the B3LYP/def2-TZVPP[22] level. Total energies of the structures that are local minima on the potential energy surface were calculated at the CCSD(T)[23]/def2-TZVPP//B3LYP/def2-TZVPP level. To gain some insights into the bonding, a natural population analysis (NPA)[24] was performed. All calculations were carried out with the Gaussian 03 program.[25]

Different energy indices have been evaluated for the ground state arrangements in order to assess their stabilities: the average binding energy (BE) was calculated using the following expression: $BE(Al_xMg_y) = [xE(Al) + yE(Mg) - E(Al_xMg_y)]/(x + y)$. In order to complement the stability evaluation of these clusters we have calculated some dissociation energies associated with the following reactions: $Al_xMg_y \rightarrow Al_x + Mg_y$; $Al_xMg_y \rightarrow Al_{x-1}Mg_y + Al$; $Al_xMg_y \rightarrow Al_xMg_{y-1} + Mg$. The energies associated with these reactions are called the fragmentation energies (FE), the aluminium abstraction energies (AE(Al)) and the magnesium abstraction energies (AE(Mg)), respectively. Here (AE(Al)) and (AE(Mg)) are the costs in energy to detach adiabatically an Al and Mg atom from the cluster, respectively.

We have computed as well the adiabatic electron affinities (EA) of the cluster as the difference between the electronic energies of the neutral and anionic cluster in their ground states ($EA = E(Al_xMg_y) - E(Al_xMg_y^-)$). Now, it is well-known that the gap between the highest occupied molecular orbital (HOMO) and the lowest unoccupied molecular orbital (LUMO), *i.e.* the HOMO–LUMO gap is directly related to the electronic stability of chemical species.[26,27] So, we have included in this report an enumeration of that parameter as well.

The phenomenological shell model (PSM) was originally developed in nuclear physics to describe the energetic ordering in the nucleus (nuclear configuration).[28] In its application to describe molecular stability, the model takes into account the possible states of a single electron confined in a potential well of a given shape.[29] PSM has been used successfully to explain qualitative electronic shell effects in size-dependent properties of simple (alkali, noble metal) clusters,[30–32] where the valence electrons of the constituent atoms can be considered itinerant. For spherical clusters, the confining potential gives rise to a spherical shell of molecular orbitals, whose shapes are similar to those of the dominant atomic orbitals.

The molecular orbital shells (called shell orbitals) are denoted by capital letters S, P, D, F, G,... corresponding to the angular momentum quantum number L = 0, 1, 2, 3, 4, ..., respectively. For a given quantum number L, the lowest shell orbital has the principal quantum number N = 1. An ideal sequence of phenomenological shell orbitals in a spherical potential is 1S, 1P, 1D, 2S, 1F, 2P, 1G, 2D, 3S, ... However, the energy ordering of the shell orbitals and the degeneracies (sub-shells) can be changed according to the potential, which depends on the details of the structural arrangement and the atomic charges.[33] According to the PSM, the clusters evolve to achieve closed electronic shells of $1S^2$, $1S^2\ 1P^6$, $1S^2\ 1P^6\ 1D^{10}$, $1S^2\ 1P^6\ 1D^{10}\ 2S^2$ and so on. So, systems with 2, 8, 18, 20, ... electrons will be the most stable.

Theoretical vertical electron detachment energies (VDEs) were calculated using two levels of theory: the Outer Valence Green Function method (ROVGF[34–38]/def2-TZVPP) and the time-dependent DFT method TD[39]-B3LYP/def2-TZVPP on the optimized B3LYP/def2-TZVPP geometries. In the time-dependent DFT framework, the first VDE was calculated as the lowest transition from the anion into the neutral cluster at the geometry of the anion. The vertical excitation energies of the neutral species in the geometry of the anion were then added to the first VDE to attain the second and higher VDEs.

Structures and bonding

In general, we find that the potential energy surfaces (PES) of the Al_xMg_y clusters are rather flat, with a variety of local minima

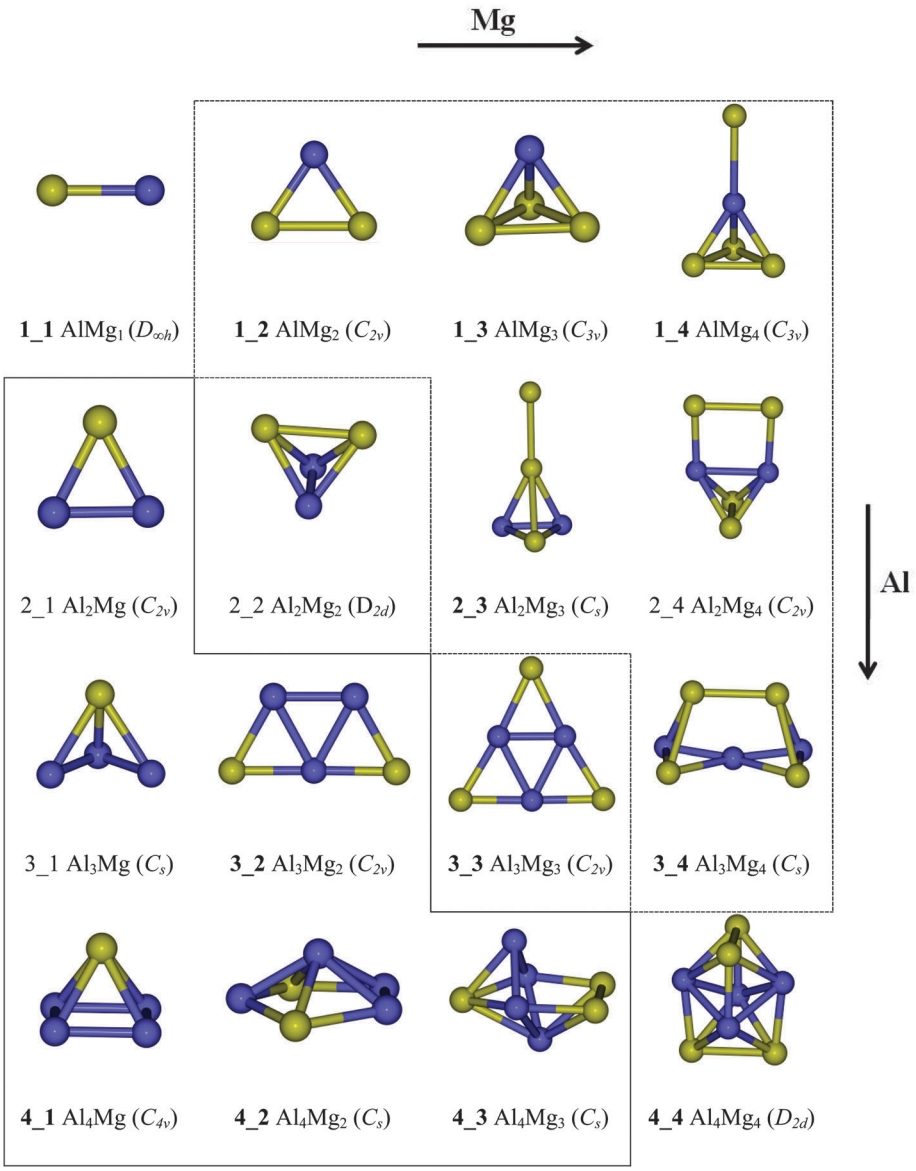

Fig. 1 Lowest energy isomers for Al_xMg_y (x, y = 1–4) at the CCSD(T)/Def2-TZVPP//B3lyp/def2-TZVPP. The blue and green spheres represent aluminium and magnesium atoms, respectively. The magnesium rich clusters are enclosed by dashed lines; the aluminium rich clusters are enclosed by solid lines.

close in energy to each other. For the full series of systems studied in this work, the most stable isomers found in the range of 10 kcal mol^{-1} relative to the global minima (at the CCSD(T)/def2-TZVPP//B3LYP/def2-TZVPP level) are listed in Fig. S1–S14 in the ESI.† All the clusters have been studied in their minimum possible multiplicities – singlet and doublet states for systems with even and odd numbers of electrons, respectively. Higher spin species are assumed to be higher in energy, which excludes further consideration after an exhaustive exploration of the PES using genetic algorithms.

The most stable isomers for each of the species are depicted in Fig. 1. The nomenclature used to identified the clusters is x_y, where x and y correspond to the numbers of Al and Mg atoms, respectively.

$AlMg_y$

Fig. 1 shows the lowest energy structures of the $AlMg_y$ clusters from y = 1 to 4 (see ESI† for the relevant Cartesian coordinates, electronic energies and zero-point corrections). The clusters in this series are doublets in their ground state conformation. For AlMg, the linear Al–Mg unit has a bond distance of 2.94 Å. Our results indicate that the most stable isomer of the $AlMg_2$ is a C_{2v} triangular 1_2 structure, with a Mg–Mg distance of 3.22 Å and an Al–Mg distance of 2.80 Å. In $AlMg_3$, the extra magnesium atom caps the $AlMg_2$ triangle forming a distorted tetrahedral structure with C_{3v} symmetry; the Al–Mg bond in this case elongates a bit to 2.84 Å while the Mg–Mg distance contracts to 3.10 Å. When the fourth Mg atom is added, it bonds to the Al atom of the distorted tetrahedron $AlMg_3$, to give rise to the

 This journal is © the Owner Societies 2013

$AlMg_4$ C_{3v} 1_4 structure (Fig. 1). The additional Mg atom perches atop the C_{3v} $AlMg_3$ fragment to form a Mg–Al bond of 3.14 Å.

Overall, in this series of clusters, one structural element appears to persist as y increases: the Mg–Al–Mg triangular structure formed by $AlMg_2$ reappears in the two higher order $AlMg_y$ clusters. The $AlMg_3$ tetrahedron also persists going from $y = 3$ to $y = 4$. However, that fragment does not appear in any of the other clusters. The fourth Mg atom seems to bond at the Al vertex of the tetrahedron rather than bonding to one of the other Mg vertices primarily because of the strength of the AlMg bond relative to the Mg–Mg interaction – not because of the stability of the $AlMg_3$ tetrahedron *per se*.

Al_2Mg_y

All of these clusters are closed shell structures. The lowest energy Al_2Mg system is a triangular C_{2v} cluster with an Al–Al distance of 2.46 Å and an Al–Mg distance of 2.76 Å, the additional Mg caps the Al_2Mg triangular face to form a distorted tetrahedral C_{2v} Al_2Mg_2 structure with an Al–Al distance of 2.67 Å and a Mg–Mg distance of 3.10 Å.

In the C_s Al_2Mg_3 cluster one Mg atom is bonded to one of the Mg atoms on the Al_2Mg_2 fragment; the latter fragment remains almost invariant and the new Mg–Mg bond distance is 3.31 Å. The Al_2Mg_4 (C_{2v} symmetry) retains the Al_2Mg_2 distorted tetrahedron fragment, but in this case one Mg_2 fragment is bonded along the Al–Al edge (see Fig. 1). Each Mg–Al distance in that planar unit is 2.81 Å and the Mg–Mg distance is 3.14 Å. In this series, the Al_2Mg triangle and later the Al_2Mg_2 pseudo-tetrahedron persist as n increases, which is in agreement with our prediction based on the PSM about the anomalous stability of the (10-electron) Al_2Mg_2 cluster.

Al_3Mg_y

The Al_3Mg cluster is a distorted tetrahedron with C_s symmetry, the Al–Al separations are 2.64 Å and 3.16 Å and the Al–Mg distances are 2.68 Å and 2.96 Å. The planar Al_3Mg_2 (C_{2v}) cluster shows a triangular Al_3 fragment capped along two edges by Mg atoms, the Al–Al and Al–Mg are 2.72 Å and 4.68 Å, respectively. The next larger cluster in the series (Al_3Mg_3) is a planar C_{2v} structure, which emerges as an Al_3 triangular fragment with three Mg atoms capping the three edges of the triangle, with Al–Al distances of 2.52 Å and 2.73 Å, and Mg–Al distances of 2.89 Å and 2.80 Å. The Al_3Mg_4 (C_s) appears as the result of capping the two outer Al_2Mg triangular sectors of the Al_3Mg_2 cluster, with a Mg atom, plus some perturbation in the resulting structure. In this series, the triangular Al_3 fragment prevails in all the clusters. As in the previously described series, the Al atoms prefer to remain coordinated among themselves – while also acting to mediate the Mg–Mg interactions. So, the Al_x sub-unit seems to typically end up in the middle of clusters where the number of Mg atoms is large enough, as in the Al_4Mg_4 and all other x_4 species.

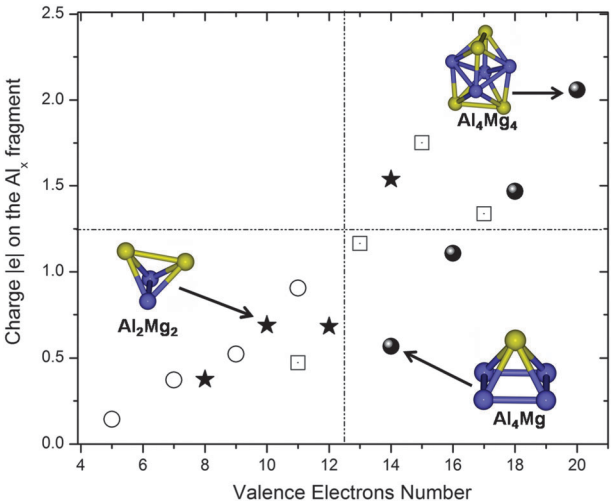

Fig. 2 The magnitude of the total NPA charges (all negative) on the Al_x fragment calculated at the B3lyp/def2-TZVPP level of theory. $AlMg_y$ [○], Al_2Mg_y [★], Al_3Mg_y [□] and Al_4Mg_y [●] (y = 1–4) clusters.

Al_4Mg_y

The Al_4Mg cluster is in fact a square planar structure defined by an Al_4 square capped by one Mg atom. The Al_4Mg_2 structure has no obvious structural relationship with Al_4Mg: in that case the global minimum is a pentagonal pyramidal form with an Al atom at the capping position. The Al_4Mg_3 could be seen as a distorted bipyramid with the new Mg atom added into the pentagon, displacing an Al atom to the open capping position. Finally the Al_4Mg_4 adopts a 3D structure with D_{2d} symmetry, where the persistent Al_4 fragment is in the central part of the structure.

To gain qualitative insight into the nature of the Al–Mg interactions in Al_xMg_y clusters, we have calculated point charges on the Al_x fragment by computing the natural population analysis (NPA).[24] As is clear from Fig. 2, the interactions present a significant amount of ionic character, the negative charge over the Al_x sub-unit increases as the number of Mg atoms increases in the clusters. However, the Mg does not donate all their valence electrons. Note that we have plotted the modulus of the negative charges in Fig. 2. The actual values are all negative. This strongly polar covalent bonding in the cluster is indeed in complete agreement with the small electronegativity differences between Al and Mg, and their metallic character.

Stability

The thermodynamic stability of the entire series of clusters was analyzed in terms of the Mg and Al abstraction energies (AE(Mg) and AE(Al), respectively); the energy change associated with the fragmentation reaction: $Al_xMg_y \rightarrow xAl + yMg$ and the binding energy divided by the number of atoms which comprise the cluster (BE). Additionally we considered two descriptors associated with the resistance of the system to changes in the electronic charge, the electron affinity (EA), and the HOMO–LUMO gap (see Fig. 3). The graphs in Fig. 3 are partitioned into

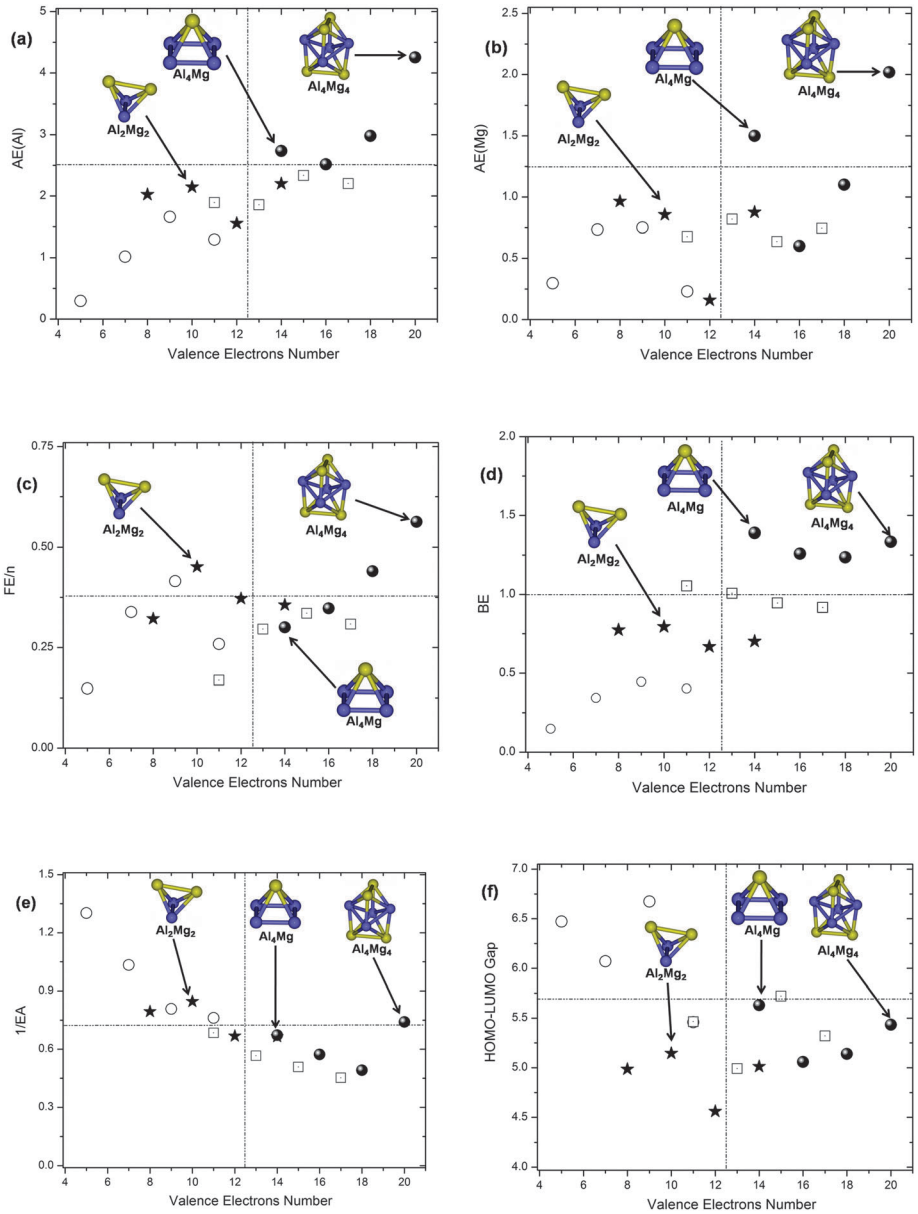

Fig. 3 Energy-based descriptors considered in comparing the thermodynamic and electronic stabilities of $AlMg_y$ [○], Al_2Mg_y [★], Al_3Mg_y [□] and Al_4Mg_y [●] (y = 1–4) clusters. In graph (c) FE/n is the magnitude of the stabilization energy per unit atom ($n = x + y$) of the Al_xMg_y cluster relative to the individual isolated Al_x and Mg_y clusters. In graph (d) BE is also an average binding energy (the binding energy per unit atom). All of the values plotted in the graphs above are in eV.

four regions. The vertical line divides the set of clusters according to their size, that is, small clusters are on the left and large clusters at the right side of the line. The horizontal lines are drawn in the middle of the graph; the systems for which the computed quantities appear above this line are expected to present quite high relative stabilities.

As shown in Fig. 3a, the AE(Al) values tend to increase as the number of Al atoms increase: Al_4Mg_4 has the largest abstraction energy and AlMg has the lowest. However, the variation in those AE values as a function of both x and y for any sub-group of clusters is quite irregular, definitely far from linear. For $AlMg_y$, for example, it is easier to remove an Al atom when y = 1 and 4, than it is to do so when y = 3. For Al_2Mg_y, however, the y = 3 case has the lowest abstraction energy. No rule seems to emerge. Indeed, the Mg abstraction energies (graph (b) in Fig. 3) are far lower and show even less ordering than the Al data.

Now, the substantial opposition of Al_4Mg and especially Al_4Mg_4 to Al removal follows the general increase in AE(Al) with x, so it is not clear from the AE(Al) data alone that the stability of that cluster is enhanced by any 'magic' electron count. However, the AE(Mg) values for Al_4Mg and Al_4Mg_4 are higher than the AE(Mg) values for all the other clusters by at least 0.5 eV, which implies a special overall stability for both clusters. The computed binding energies (Fig. 3d) are also highest for those two species and the fragmentation energy per atom, (Fig. 3c), which is a normalized value ignoring the differences in the valence structure of Al *vs.* Mg

 This journal is © the Owner Societies 2013

is still far larger for Al_4Mg_4. Put another way, the Al_4Mg_4 is the most resistant cluster in the entire series to fragmentation. In the smaller cluster regime, Al_2Mg_2 is the most stable.

For the smaller clusters, the AlMg and the $AlMg_2$ are the most resistant to reduction (higher 1/EA, Fig. 3e). In general the EA increases as the cluster size increases, but there is a prominent discontinuity at Al_4Mg_4; the latter is the most stable cluster in the region of the larger clusters against reduction – which is in total agreement with the character of the closed shell system in the PSM model.

Another electronic structure based descriptor associated with the electronic stability of clusters is the HOMO–LUMO gap. Large values for such gaps are typically indicative of relatively high thermodynamic stability in compounds. In this case, the stable systems predicted based on simple electron counting rules (such as Al_2Mg_2, Al_4Mg, and Al_4Mg_4) do not present the highest gaps along the complete series. This may be due to the increase in the metallic character of the system as the clusters size increases such that the HOMO–LUMO gap reduction indicates an incremental move towards metallicity. So the gap can, unfortunately, not be used to explain stability across systems of very different sizes. It should be noted, however, that those three clusters present relatively high gaps compared to the other systems neighboring them in the specific Al_2Mg_y and Al_4Mg_y series (Fig. 3f).

Molecular orbital and PSM analysis of Al_4Mg, Al_2Mg_2 and Al_4Mg_4

The global minimum energy isomer of Al_4Mg (C_{4v}) is a pyramidal structure in agreement with the theoretical prediction of Mandado *et al.*[14] This system could be viewed as one Al_4^{2-} ring stabilized by the counter-ion Mg^{2+}. The NPA analysis previously discussed shows that interaction between Mg and the Al_4 ring is indeed quite ionic, with a net charge on the Al_4 ring of approximately $-0.60e$. The Al_4^{2-} ion has been exhaustively studied both theoretically and experimentally and its stability has been attributed to the presence of σ and π aromatic character.[9,40]

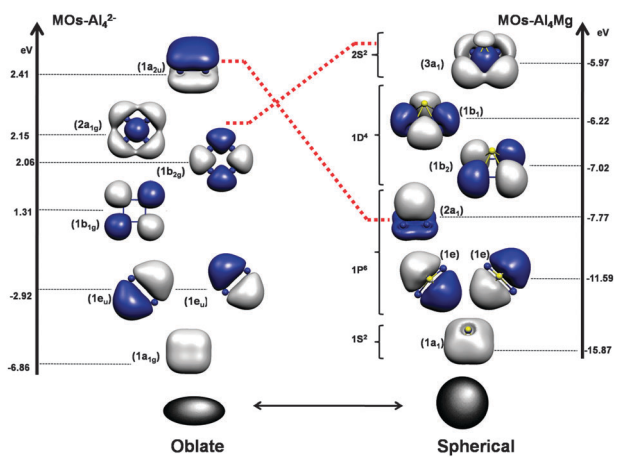

Fig. 4 Molecular orbital pictures and the electronic shell assignation according to PSM.

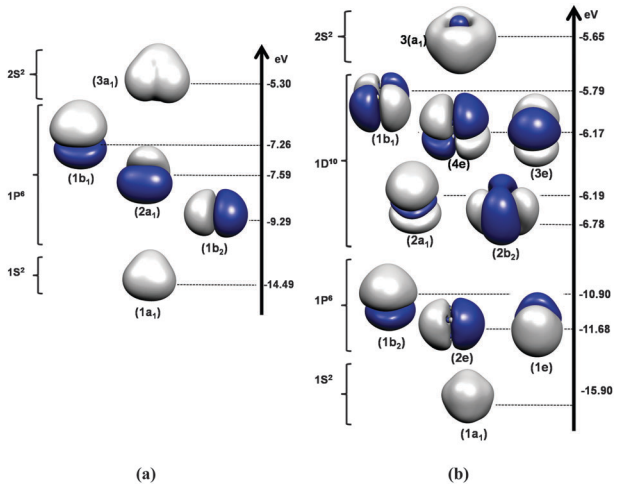

Fig. 5 Molecular orbital pictures and the electronic shell assignation according to PSM. (a) Al_2Mg_2 and (b) Al_4Mg_4

The molecular orbitals of Al_4^{2-} and Al_4Mg are compared in Fig. 4. In the PSM model, the shell becomes closed when all the three P or all the five D orbitals are filled with 6 or 10 electrons, respectively, and the system adopts a nearly spherical shape. However, when these shells are partially occupied, the electronic structure can lead to Jahn–Teller distortions, generating low symmetry structures. Clemenger exhaustively analyzed this situation[41] adapting the Nilsson model to (reference) metal clusters (called the Clemenger–Nilsson model, CNM). This model is an extension of the PSM, but is not restricted to spherical systems. According to the model, the oblate shape stabilizes the orbitals which have no *xy* nodal plane, like P_x,P_y,D_{xy},$D_{x^2-y^2}$, and destabilizes the orbitals which have such planes, like P_z and D_{z^2}. As is shown in Fig. 4, the Al_4^{2-} orbitals should correspond to a highly distorted oblate cluster shape. Nevertheless, in the case of the Al_4Mg the structure of the system evolves to a spherical shape, which leads to changes in the electronic configuration; the P_z orbital is stabilized (red dotted lines in Fig. 4) due to the changes in the confining potential by the inclusion of the Mg into the structure.

Looking at the shapes of the valence-MOs and the ordering of the energy levels allows us to rationalize the stabilities of Al_2Mg_2 and Al_4Mg_4 using the phenomenological shell model (PSM). The electronic shell configurations of the clusters in this model should be:

$$Al_2Mg_2 \rightarrow 1S^2 1P^6 2S^2 \text{ and } Al_4Mg_4 \rightarrow 1S^2 1P^6 1D^{10} 2S^2$$

From Fig. 5, it is apparent that the valence molecular orbitals in Al_2Mg_2 and Al_4Mg_4 resemble atomic orbital shapes and the energy ordering is in agreement with the PSM. So, the relative stabilities of these clusters are in agreement with the expected closed shell configuration in the PSM.

Photoelectron spectroscopy of $Al_4Mg_4^-$

A consensus among the stability descriptors suggests that Al_4Mg_4 is the most stable among the studied clusters. It presents a closed shell (20 valence electrons) highly stable

Table 1 Theoretical VDEs (eV) for the two lowest energy isomers of $Al_4Mg_4^-$ (ΔE = 0.0 and 2.3 kcal mol^{-1})

Cluster	Final state and electronic configuration		UOVGF[a]	TD-B3LYP[b]
4A-1 $Al_4Mg_4^-$ (D_{2d}) $^2B_2$ (0.0)	$^1A_1$	$1a_2^2 1e^4 1b_2^2 2a_1^2 2b_2^2 2e^4 1b_1^2 3a_1^2 3b_2^0$	1.56 (0.90)	1.52
	$^3B_2$	$1a_2^2 1e^4 1b_2^2 2a_1^2 2b_2^2 2e^4 1b_1^2 3a_1^1 3b_2^1$	2.58 (0.86)	2.48
	$^1B_2$	$1a_2^2 1e^4 1b_2^2 2a_1^2 2b_2^2 2e^4 1b_1^2 3a_1^1 3b_2^1$	[c]	2.59
	$^3A_2$	$1a_2^2 1e^4 1b_2^2 2a_1^2 2b_2^2 2e^4 1b_1^1 3a_1^2 3b_2^1$	2.59 (0.86)	2.56
	$^1A_2$	$1a_2^2 1e^4 1b_2^2 2a_1^2 2b_2^2 2e^4 1b_1^1 3a_1^2 3b_2^1$	[c]	2.57
	^3E	$1a_2^2 1e^4 1b_2^2 2a_1^2 2b_2^2 2e^3 1b_1^2 3a_1^2 3b_2^1$	2.83 (0.85)	2.92
	^1E	$1a_2^2 1e^4 1b_2^2 2a_1^2 2b_2^2 2e^3 1b_1^2 3a_1^2 3b_2^1$	[c]	3.08
	$^3A_1$	$1a_2^2 1e^4 1b_2^2 2a_1^2 2b_2^1 2e^4 1b_1^2 3a_1^2 3b_2^1$	2.96 (0.85)	3.14
	$^1A_1$	$1a_2^2 1e^4 1b_2^2 2a_1^2 2b_2^1 2e^4 1b_1^2 3a_1^2 3b_2^1$	[c]	3.58
4A-2 $Al_4Mg_4^-$ (C_s) $^2A'$ (2.3)	$^1A'$	$1a'^2 2a'^2 1a''^2 3a'^2 4a'^2 2a''^2 5a'^2 6a'^2 7a'^2 3a''^2 8a'^0$	1.88 (0.90)	1.69
	$^3A''$	$1a'^2 2a'^2 1a''^2 3a'^2 4a'^2 2a''^2 5a'^2 6a'^2 7a'^2 3a''^1 8a'^1$	2.44 (0.86)	2.41
	$^1A''$	$1a'^2 2a'^2 1a''^2 3a'^2 4a'^2 2a''^2 5a'^2 6a'^2 7a'^2 3a''^1 8a'^1$	[c]	2.47
	$^3A'$	$1a'^2 2a'^2 1a''^2 3a'^2 4a'^2 2a''^2 5a'^2 6a'^2 7a'^1 3a''^2 8a'^1$	2.51 (0.86)	2.44
	$^1A'$	$1a'^2 2a'^2 1a''^2 3a'^2 4a'^2 2a''^2 5a'^2 6a'^2 7a'^1 3a''^2 8a'^1$	[c]	2.61
	$^3A'$	$1a'^2 2a'^2 1a''^2 3a'^2 4a'^2 2a''^2 5a'^2 6a'^1 7a'^2 3a''^2 8a'^1$	2.88 (0.85)	2.96
	$^1A'$	$1a'^2 2a'^2 1a''^2 3a'^2 4a'^2 2a''^2 5a'^2 6a'^1 7a'^2 3a''^2 8a'^1$	[c]	3.13
	$^3A'$	$1a'^2 2a'^2 1a''^2 3a'^2 4a'^2 2a''^2 5a'^1 6a'^2 7a'^2 3a''^2 8a'^1$	3.01 (0.86)	3.06
	$^1A'$	$1a'^2 2a'^2 1a''^2 3a'^2 4a'^2 2a''^2 5a'^1 6a'^2 7a'^2 3a''^2 8a'^1$	[c]	3.26

[a] The VDEs were calculated at the UOVGF/def2TZVPP//B3LYP/def2TZVPP level of theory. [b] The VDEs were calculated using the TD-B3LYP/def2TZVPP//B3LYP/def2TZVPP. [c] The VDEs in the final singlet states were not calculated because of the multi-configurational nature of the final singlet state.

electronic structure in the PSM. Given that the structures reported in this work (Fig. 1) are global minima on their corresponding potential energy surfaces, we propose them as good candidates for experimental detection.

In that context, it is important to provide theoretical predictions that could be compared with experimental data in the future. The predictions reported here were evaluated in monoanionic species, which are the typical targets of photoelectron spectroscopic experiments on clusters. We have explored the energy surfaces for all of the anionic species of the evaluated clusters, and the global minimum energy structures are reported in the ESI.†

Among the various experimental methods of analysis for studying mass-selected clusters, photoelectron spectroscopy has attracted attention due to the possibility of studying electronic properties of clusters as well as vibrational fine structures.[42–45] We have calculated the VDEs for the $Al_4Mg_4^-$ in their two lowest-lying isomers **4A-1** and **4A-2** (ΔE = 0.0 and 2.3 kcal mol^{-1}, see ESI†), which are summarized in Table 1, where the calculated VDEs at various levels of theory are listed. These VDEs should correspond to the maximum values of each experimental photoelectron spectra, and could be used to assign the corresponding structures.

The first peak for **4A-1** and **4A-2** should be at about 1.6 and 1.9 eV, respectively, while the second peak should be at about 2.6 and 2.4 eV, respectively. The gap between the first and the second VDEs for **4A-1** and **4A-2** is 1.0 and 0.5 eV, respectively. The spectra of **4A-1** and **4A-2** may present a very broad band, which also contains two overlapping detachment transitions (second and third peaks), where the differences between two signals, for the two isomers, are small. The forth and fifth peaks for **4A-1** should be at about 2.8 and 3.0 eV, respectively, while the forth and fifth peak for **4A-2** are essentially at the same position (3.0 and 3.0 eV). So, the gap between the first and the second VDEs for **4A-1** and **4A-2** may be important for the assignment of the structure in the experimental photoelectron spectrum of $Al_4Mg_4^-$.

Concluding remarks

We have explored in detail the potential energy surfaces of the Al_xMg_y (x,y = 1–4) series of clusters. We find that Al_4Mg, Al_2Mg_2 and Al_4Mg_4 present high relative stabilities according to a set of theoretical descriptors used in the analysis. In the case of the Al_4Mg structure we find that the electronic configuration is similar to that of the Al_4^{2-} system, which is an aromatic species according to the $4n + 2$ rule of planar rings. Our analysis of the electronic configuration of the Al_4Mg indicates a connection between this polar covalent structure in the phenomenological shell model (PSM) and the $4n + 2$ rule. The clusters Al_2Mg_2 and Al_4Mg_4 form stable 3D structures, and their stability are rationalized as a consequence of their closed shell nature in terms of the PSM, with 10 and 20 itinerant electrons respectively. The VDEs for the monoanionic species derived from the $Al_4Mg_4^- \rightarrow Al_4Mg_4 + 1e^-$ are reported with the purpose of providing predictive data for future experimental verification.

Acknowledgements

Our work was supported by Fondecyt (Grants No. 11090431 and No. 3130500). The work at the University of Antioquia was funded by the "Sostenibilidad" Program 2012–2013. At Universidad de Medellin, the work was supported by the project No. 626. At the University of Richmond, KJD gratefully acknowledges the National Science Foundation for funding under (NSF-CAREER) CHE-1056430.

References

1 A. W. Castleman and S. N. Khanna, *J. Phys. Chem. C*, 2009, **113**, 2664–2675.
2 S. A. Claridge, A. W. Castleman Jr., S. N. Khanna, C. B. Murray, A. Sen and P. S. Weiss, *Acs Nano*, 2009, **3**, 244–255.

 This journal is © the Owner Societies 2013

3 P. Jena and S. N. Khanna, *Mater. Sci. Eng., A*, 1996, **217–218**, 218–222.
4 A. Perez, P. Melinon, V. Dupuis, P. Jensen, B. Prevel, J. Tuaillon, L. Bardotti, C. Martet, M. Treilleux, M. Broyer, M. Pellarin, J. L. Vaille, B. Palpant and J. Lerme, *J. Phys. D: Appl. Phys.*, 1997, **30**, 709–721.
5 A. Varano, D. J. Henry and I. Yarovsky, *J. Phys. Chem. A*, 2010, **114**, 3602–3608.
6 E. Hückel, *Zeitschrift für Physik A Hadrons and Nuclei*, 1931, **70**, 204–286.
7 E. Hückel, *Zeitschrift für Physik A Hadrons and Nuclei*, 1931, **72**, 310–337.
8 E. Hückel, *Zeitschrift für Physik A Hadrons and Nuclei*, 1932, **76**, 628–648.
9 X. Li, A. E. Kuznetsov, H. F. Zhang, A. I. Boldyrev and L. S. Wang, *Science*, 2001, **291**, 859–861.
10 P. W. Fowler and D. E. Manolopoulos, *An atlas of fullerenes*, Clarendon Press, 1995.
11 A. Hirsch, Z. Chen and H. Jiao, *Angew. Chem., Int. Ed.*, 2000, **39**, 3915–3917.
12 P. K. Chattaraj, *Aromaticity and Metal Clusters*, CRC Press, 2010.
13 (*a*) W. Tiznado, N. Perez-Peralta, R. Islas, A. Toro-Labbe, J. M. Ugalde and G. Merino, *J. Am. Chem. Soc.*, 2009, **131**, 9426–9431; (*b*) E. Osorio, V. Villalobos, J. C. Santos, K. J. Donald, G. Merino and W. Tiznado, *Chem. Phys. Lett.*, 2012, **522**, 67–71; (*c*) J. C. Santos, M. Contreras and G. Merino, *Chem. Phys. Lett.*, 2010, **496**, 172–174.
14 M. Mandado, A. Krishtal, C. Van Alsenoy, P. Bultinck and J. M. Hermida-Ramon, *J. Phys. Chem. A*, 2007, **111**, 11885–11893.
15 A. N. Alexandrova and A. I. Boldyrev, *J. Chem. Theory Comput.*, 2005, **1**, 566–580.
16 A. N. Alexandrova, A. I. Boldyrev, Y. J. Fu, X. Yang, X. B. Wang and L. S. Wang, *J. Chem. Phys.*, 2004, **121**, 5709–5719.
17 A. N. Alexandrova, *J. Phys. Chem. A*, 2010, **114**, 12591–12599.
18 A. D. Becke, *Phys. Rev. A: At., Mol., Opt. Phys.*, 1988, **38**, 3098–3100.
19 C. T. Lee, W. T. Yang and R. G. Parr, *Phys. Rev. B: Condens. Matter Mater. Phys.*, 1988, **37**, 785–789.
20 P. Fuentealba, H. Preuss, H. Stoll and L. von Szentpály, *Chem. Phys. Lett.*, 1982, **89**, 418–422.
21 P. Fuentealba, L. von Szentpály, H. Preuss and H. Stoll, *J. Phys. B:At., Mol. Opt. Phys.*, 1985, **18**, 1287–1296.
22 F. Weigend and R. Ahlrichs, *Phys. Chem. Chem. Phys.*, 2005, **7**, 3297–3305.
23 J. A. Pople, M. Head-Gordon and K. Raghavachari, *J. Chem. Phys.*, 1987, **87**, 5968–5975.
24 A. E. Reed, R. B. Weinstock and F. Weinhold, *J. Chem. Phys.*, 1985, **83**, 735–746.
25 M. J. Frisch, G. W. Trucks, H. B. Schlegel, G. E. Scuseria, M. A. Robb, J. R. Cheeseman, J. A. Montgomery, T. Vreven, K. N. Kudin, J. C. Burant, J. M. Millam, S. S. Iyengar, J. Tomasi, V. Barone, B. Mennucci, M. Cossi, G. Scalmani, N. Rega, G. A. Petersson, H. Nakatsuji, M. Hada, M. Ehara, K. Toyota, R. Fukuda, J. Hasegawa, M. Ishida, T. Nakajima, Y. Honda, O. Kitao, H. Nakai, M. Klene, X. Li, J. E. Knox, H. P. Hratchian, J. B. Cross, V. Bakken, C. Adamo, J. Jaramillo, R. Gomperts, R. E. Stratmann, O. Yazyev, A. J. Austin, R. Cammi, C. Pomelli, J. W. Ochterski, P. Y. Ayala, K. Morokuma, G. A. Voth, P. Salvador, J. J. Dannenberg, V. G. Zakrzewski, S. Dapprich, A. D. Daniels, M. C. Strain, O. Farkas, D. K. Malick, A. D. Rabuck, K. Raghavachari, J. B. Foresman, J. V. Ortiz, Q. Cui, A. G. Baboul, S. Clifford, J. Cioslowski, B. B. Stefanov, G. Liu, A. Liashenko, P. Piskorz, I. Komaromi, R. L. Martin, D. J. Fox, T. Keith, A. Laham, C. Y. Peng, A. Nanayakkara, M. Challacombe, P. M. W. Gill, B. Johnson, W. Chen, M. W. Wong, C. Gonzalez and J. A. Pople, *Gaussian 03, Revision E.01*, Gaussian, Inc., Wallingford CT, 2004.
26 P. Geerlings, F. De Proft and W. Langenaeker, *Chem. Rev.*, 2003, **103**, 1793–1874.
27 R. G. Pearson, *Acc. Chem. Res.*, 1993, **26**, 250–255.
28 M. G. Mayer and J. H. D. Jensen, *Elementary Theory of Nuclear Shell Structure*, John Wiley and Sons, New York, 1955.
29 W. D. Knight, K. Clemenger, W. A. de Heer, W. A. Saunders, M. Y. Chou and M. L. Cohen, *Phys. Rev. Lett.*, 1984, **52**, 2141–2143.
30 M. Brack, *Rev. Mod. Phys.*, 1993, **65**, 677–732.
31 W. A. de Heer, *Rev. Mod. Phys.*, 1993, **65**, 611–676.
32 T. Holtzl, P. Lievens, T. Veszpremi and N. Minh Tho, *J. Phys. Chem. C*, 2009, **113**, 21016–21018.
33 E. Janssens, S. Neukermans and P. Lievens, *Curr. Opin. Solid State Mater.Sci.*, 2004, **8**, 185–193.
34 L. S. Cederbaum, *J. Phys. B: At. Mol. Phys.*, 1975, **8**, 290.
35 J.-S. Lin and J. V. Ortiz, *Chem. Phys. Lett.*, 1990, **171**, 197–200.
36 W. von Niessen, J. Schirmer and L. S. Cederbaum, *Comput. Phys. Rep.*, 1984, **1**, 57–125.
37 V. G. Zakrzewski and J. V. Ortiz, *Int. J.Quantum Chem.*, 1995, **53**, 583–590.
38 V. G. Zakrzewski, J. V. Ortiz, J. A. Nichols, D. Heryadi, D. L. Yeager and J. T. Golab, *Int. J. Quantum Chem.*, 1996, **60**, 29–36.
39 R. Bauernschmitt and R. Ahlrichs, *Chem. Phys. Lett.*, 1996, **256**, 454–464.
40 A. I. Boldyrev and L. S. Wang, *Chem. Rev.*, 2005, **105**, 3716–3757.
41 K. Clemenger, *Phys. Rev. B: Condens. Matter Mater. Phys.*, 1985, **32**, 1359–1362.
42 D. M. Neumark, *Annu. Rev. Phys. Chem.*, 2001, **52**, 255–277.
43 K. Rademann, *Phys. Chem. Chem. Phys.*, 1989, **93**, 653–670.
44 A. Stolow, A. E. Bragg and D. M. Neumark, *Chem. Rev.*, 2004, **104**, 1719–1757.
45 L. S. Wang and X. B. Wang, *J. Phys. Chem. A*, 2000, **104**, 1978–1990.